

The Milky Way’s rotation curve with superfluid dark matter

Sabine Hossenfelder, Tobias Mistle

*Frankfurt Institute for Advanced Studies
Ruth-Moufang-Str. 1, D-60438 Frankfurt am Main, Germany*

Abstract

Recent studies have shown that dark matter with a superfluid phase in which phonons mediate a long-distance force gives rise to the phenomenologically well-established regularities of Modified Newtonian Dynamics (MOND). Superfluid dark matter, therefore, has emerged as a promising explanation for astrophysical observations by combining the benefits of both particle dark matter and MOND, or its relativistic completions, respectively.

We here investigate whether superfluid dark matter can reproduce the observed Milky Way rotation curve for $R < 25$ kpc and are able to answer this question in the affirmative. Our analysis demonstrates that superfluid dark matter fits the data well with parameters in reasonable ranges. The most notable difference between superfluid dark matter and MOND is that superfluid dark matter requires about 20% less total baryonic mass (with a suitable interpolation function). Our analysis further allows us to estimate the radius of the Milky Way’s superfluid core and the total mass of dark matter in both the superfluid and the normal phase.

1 Introduction

Astrophysics has a big problem. Simply combining General Relativity with the matter-content of the Standard Model of particle physics does not correctly describe a variety of observations, ranging from the cosmic microwave background to galaxy clusters, to individual galaxies. The common remedy for this mismatch between theory and data is to conjecture a new type of matter – “dark matter” – which is presumably made of particles that so-far evaded direct detection.

However, in the past two decades it has become increasingly clear that particle dark matter has its own problems, problems that are particularly obvious on galactic scales. The reason is that once one conjectures the properties of a particular type of dark matter particles, computer simulations should reveal how these particles form structures. The so-obtained structures, however, do not readily agree with observational evidence. The core-cusp problem [1] and the missing dwarf galaxies [2, 3] are the most widely-known

problems with the dark matter paradigm, though by far not the only ones [4]. These discrepancies between the dark matter models and the galactic structures may be due to shortcomings in the numerical calculations or they may signal a severe theoretical shortcoming. Either way, they mean we do not know the correct explanation.

Even more worrying than the difficulty of reproducing galaxies-as-observed is what dark matter does not predict, notably the baryonic Tully-Fisher relation [5] and the Radial Acceleration Relation [6]. It also does not lend credibility to the dark matter hypothesis that to date all attempts to directly detect the hypothetical particles have failed [7].

A promising, alternative explanation for the puzzling astrophysical observations has been around since the mid 1980s. Its original formulation has become known as Modified Newtonian Dynamics (MOND) [8–10]. The idea of MOND is simple: Instead of increasing the gravitational pull by adding a new type of invisible matter, increase the gravitational pull of the normal matter by altering the force.

It must be emphasized that MOND is a phenomenological model that is strictly speaking wrong. It is not relativistically invariant and non-local in the same way that Newtonian gravity is non-local. MOND therefore must be understood as an approximation that has to be completed to give a fully-relativistic theory of modified gravity.

A variety of such relativistic completions of MOND have been proposed in the literature [11–17], but they face a common problem. While modifications of gravity are superior on galactic scales because of their parametric simplicity, on larger scales dark matter is the simpler explanation. This tension between the cosmological and galactic scales can be resolved with any theory that combines cold dark matter for the former case and a MOND-limit for the latter. A strong contender for just such a theory which has recently emerged is superfluid dark matter (hereafter: SFDM).

The idea that dark matter may have a superfluid phase is itself not new [18–27], but the type of superfluid dark matter we are concerned with here is novel because it generates a long-range force. This force stems from the exchange of phonons between (effective) particles of normal matter and it reproduces the force-law of MOND. If the superfluid phase however breaks down – because the pressure is too low or the temperature too high – then the matter will behave like common-type particle dark matter. One then has to find a suitable type of particle for which a superfluid exists in galaxies, but not in intergalactic space or in the early universe.

It was shown in [28, 29] that one can combine the successes of MOND on galactic scales with the successes of Λ CDM on cosmological scales by choosing an axion-like particle with a mass in the range of $\approx 1\text{eV}$. Besides the mass of the particle, the free parameters of this model are the self-interaction strength of the new particle (which has to generate a superfluid) and the strength of its interaction with baryonic matter. We know from the observation of a gravitational wave event with an electromagnetic counterpart [30] that the coupling of the superfluid to photons must be very small and we will therefore here set it to zero.

This SFDM is still young and how well it will fare for large-scale structure forma-

tion is not presently known. It has been shown however that superfluid dark matter can correctly reproduce rotation curves for a large variety of galaxies by the same mechanism that MOND does. For the same reason this model can explain the Tully-Fisher relation. In [31] it was furthermore demonstrated the SFDM has no difficulties reproducing both the strong gravitational lensing data and the kinematic measurements for stellar rotation.

On purely mathematical grounds, SFDM holds a middle-position between modified gravity and particle dark matter. This is because in general both types of theories add new quantum fields to the currently accepted fundamental laws that are General Relativity and the Standard Model of particle physics. Whether these fields are to be interpreted as belonging to the gravitational part or to the matter part is ambiguous and requires further definition. In SFDM, the major contribution to the (inferred) long-range force acting on normal matter is *not* the normal, general-relativistic gravitational pull of the superfluid, but rather the new phonon-force. Because of this property, SFDM can rightfully be said to be a modification of gravity rather than a type of dark matter. However, the particles that make up the superfluid of course also have a gravitational pull, so really one necessarily has a combination of both.

Indeed, it was shown in [17] that making the theory of emergent gravity proposed in [32] generally covariant gives rise to a Lagrangian very similar to that of SFDM. This is not surprising because both reproduce the MOND-limit, but it serves to show that the equations we will be dealing with here can reasonably be thought of as both, a modification of gravity and an addition to the matter sector.

However, our aim here is not to interpret the equations but to investigate whether they are useful to describe observations. In particular, the purpose of this present work is to investigate whether the SFDM model can appropriately reproduce the rotation curve of our own galaxy. While the Milky-Way is only one galaxy of many, it has the benefit that its rotation curve has been measured to excellent accuracy [33, 34], so much so that the most recent data is sensitive to the detailed mass distribution of the spiral arms. Our analysis here will be similar to that provided in [35] for the Radial Acceleration Relation in MOND.

This paper is organized as follows. In Section 2 we briefly summarize the key properties of superfluid dark matter and recall its relation to MOND. In Section 3 we explain what data we are using. In Section 4 we detail how we integrate the equations and match them to the data. Results are presented in section 5. After a short discussion in Section 6 we conclude in Section 7.

2 Superfluid Dark Matter

Following the notation of [28], we describe the superfluid by a massive scalar field with phase θ . In the condensed phase the field associated with the phase is to good approximation classical. In the non-relativistic limit, the equations for the condensate are then

[29, 36]:

$$\Delta \left(-\frac{\hat{\mu}}{m} \right) = 4\pi G \left(\rho_b + \rho_{\text{SF}} \left(\hat{\mu}, (\vec{\nabla}\theta)^2 \right) \right), \quad (1a)$$

$$\vec{\nabla} \left(\frac{(\vec{\nabla}\theta)^2 + 2m(\frac{2\beta}{3} - 1)\hat{\mu}}{\sqrt{(\vec{\nabla}\theta)^2 + 2m(\beta - 1)\hat{\mu}}} \vec{\nabla}\theta \right) = \frac{\alpha}{2M_{\text{Pl}}} \rho_b, \quad (1b)$$

where

$$\rho_{\text{SF}} \left(\hat{\mu}, (\vec{\nabla}\theta)^2 \right) = \frac{2\sqrt{2}}{3} m^{5/2} \Lambda \frac{3(\beta - 1)\hat{\mu} + (3 - \beta) \frac{(\vec{\nabla}\theta)^2}{2m}}{\sqrt{(\beta - 1)\hat{\mu} + \frac{(\vec{\nabla}\theta)^2}{2m}}}. \quad (2)$$

Here, ρ_{SF} is the energy-density of the superfluid and ρ_b is the energy-density of baryons whose profile we extract from data as described in Sec. 3. m is the mass of the superfluid's constituent particles, and $\hat{\mu} = \mu_{\text{nr}} - m\phi_N$ is a combination of the non-relativistic chemical potential μ_{nr} (a constant that acts as initial value) and the Newtonian gravitational potential ϕ_N . Expressed in these terms, Eq. (1a) is the usual Poisson equation for the Newtonian gravitational potential and Eq. (1b) determines SFDM's phonon field θ that carries the MOND-like force.

In the above equations, M_{Pl} denotes the Planck mass, α is a dimensionless coupling constant, and Λ is related to the self-interaction strength of the new field [28]. The parameter β quantifies finite-temperature corrections as discussed in Ref. [28].

In SFDM, the baryons' total acceleration \vec{a}_{tot} is then a sum of the acceleration from the Newtonian gravitational pull due to the baryonic and superfluid mass densities, \vec{a}_N , and the acceleration from the phonon force, \vec{a}_θ , which is proportional to the gradient $\vec{\nabla}\theta$:

$$\vec{a}_{\text{tot}} = \vec{a}_N + \vec{a}_\theta = -\vec{\nabla}\phi_N - \frac{\alpha\Lambda}{M_{\text{Pl}}} \vec{\nabla}\theta. \quad (3)$$

In our below analysis, we will further consider an idealized MOND-limit to highlight the differences between the two models. In this MOND-limit, we neglect the energy-density of the superfluid and assume that the kinetic energy of the phonon field is much larger than the chemical potential $|\vec{\nabla}\theta|^2/(2m) \gg \hat{\mu}$. In this case, the equations simplify to

$$\Delta\phi_N = 4\pi G \rho_b, \quad (4a)$$

$$\vec{\nabla} \left(\left(\frac{\sqrt{(\vec{\nabla}\bar{\theta})^2}}{a_{0,\theta}} \right) \vec{\nabla}\bar{\theta} \right) = 4\pi G \rho_b, \quad (4b)$$

where we introduced the parameters $\bar{\theta} = (\alpha\Lambda/M_{\text{Pl}})\theta$, $a_{0,\theta} = \alpha^3\Lambda^2/M_{\text{Pl}}$, and $8\pi G = M_{\text{Pl}}^{-2}$ to match the expressions to the common MOND-formalism.

MOND further requires an interpolation function whose purpose is to fade out the regime of Newtonian gravity and cross over to the new, logarithmic potential law. This interpolation function is defined as the scalar function that, when multiplied with the acceleration from the Newtonian gravitational pull of the normal matter gives the total acceleration in MOND. This interpolation function corresponds to the phenomenologically obtained Radial Acceleration Relation (RAR)¹. Strictly speaking, this is correct only in the no-curl approximation, see Section 4. However, we show in Section 5.1 that the no-curl approximation is good to use, and hence the use of the radial acceleration relation justified.

An interpolation function is not necessary in SFDM, but to compare our results to those obtained with MOND, we use the exponential MOND interpolation function

$$\nu_e(y) = \frac{1}{1 - e^{-\sqrt{y}}}, \quad (5)$$

where $y = a_b/a_{0,e}$ with the Newtonian baryonic acceleration a_b and the acceleration scale $a_{0,e} = 1.2 \cdot 10^{-10} \text{ m/s}^2$.

As laid out in [36], in the idealized MOND-limit, SFDM is equivalent to MOND with the interpolation function

$$\nu_\theta(y) = 1 + \frac{1}{\sqrt{y}}, \quad (6)$$

where $y = a_b/a_{0,\theta}$ and the acceleration scale is $a_{0,\theta} = 0.87 \cdot 10^{-10} \text{ m/s}^2$ for the fiducial parameter values from Ref. [29]. Again, this equivalence strictly speaking only holds in the no-curl-approximation, because the curl-terms in the SFDM model are different from those of MOND even in the idealized MOND-limit. However, as we will see later, the difference is negligible for fitting the data we will be dealing with. In the non-idealized case, SFDM cannot be cast into the form of an interpolation function both because of the superfluid's gravitational pull and because the phonon force is not exactly of the MOND form.

3 Data

Recently, Ref. [35] put forward a new model for the Milky Way (MW) to match the most up-to-date terminal velocity data. It provides an excellent fit to the MW's rotation curve even outside the range where this model was fitted. This model relates the Newtonian acceleration from the baryonic mass distribution with the total acceleration by employing the Radial Acceleration Relation from Ref. [6].

We take the baryonic mass distribution from Ref. [35] with a few minor modifications. Our model consists of a bulge, a gas disk, and a stellar disk. We take the stellar

¹We wish to emphasize that with Radial Acceleration Relation we refer to the relation between the radial accelerations in general, not to the fit of this relation with a specific interpolation function.

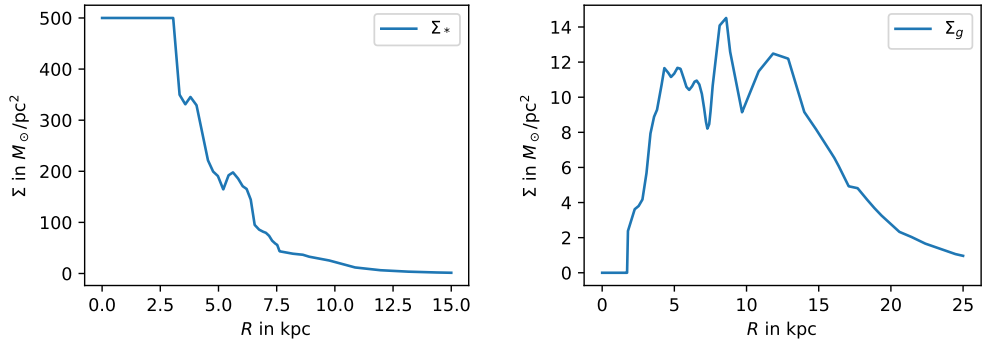


Figure 1: Left: Numerical stellar surface density Σ_* from Ref. [35]. Right: Numerical gas surface density Σ_g from Ref. [35].

disk exactly as in Ref. [35], i.e. we use a scale height of 300 pc with the numerical surface density from Ref. [35]. For the gas disk, we also use the numerical surface density from Ref. [35]. However, following Ref. [37], we use a disk with scale height 130 pc instead of an infinitely thin disk because a finite height is easier to handle with our numerical code. The choice of this scale height does not significantly affect our results.

The gas surface density is that of Ref. [38], but scaled up by a factor of 1.4 to account for helium and metals, and adjusted for newer measurements of the Galactic size R_0 [39], see Refs. [35, 40] for details. The resulting gas surface density, which is not a smooth exponential, is shown in Fig. 1, left.

The stellar surface density is based on a Freeman Type II profile [41] that was adjusted to fit the detailed terminal velocity data for $3 \text{ kpc} < R < 8 \text{ kpc}$, see Ref. [35]. The resulting profile is shown in Fig. 1, right.

The bulge profile is parameterized as [40]

$$\rho_{\text{bulge}}(b) = \frac{\rho_{\text{bulge},0}}{\eta\zeta b_m^3} \frac{\exp[-(b/b_m)^2]}{(1+b/b_0)^{1.8}}, \quad (7)$$

where $\eta = 0.5$, $\zeta = 0.6$, $b_m = 1.9 \text{ kpc}$, $b_0 = 0.1 \text{ kpc}$, and $b = r/(\eta\zeta)^{1/3}$ with the spherical radius r . This is the spherically equivalent mass distribution of the triaxial model used in Ref. [35]. The constant $\rho_{\text{bulge},0}$ is chosen such that the asymptotic Newtonian acceleration due to the bulge is the same as in Ref. [35], see Table 2 there.

In the following, we keep the shape of the baryonic mass distribution fixed, but allow to rescale the baryonic mass distribution as a whole in order to fit the MW rotation curve. For this, we introduce the parameter f_b that multiplies the baryonic mass distribution $\rho_b(R, z)$. Here, R and z are the usual cylindrical coordinates.

We take the MW rotation curve data from Ref. [35]. That is, we take the rotation curve data from Ref. [34] for $R > 5 \text{ kpc}$ and from Ref. [42] for $R < 2.2 \text{ kpc}$, but with

two adjustments made in Ref. [35]: The Jeans analysis in Ref. [34] assumes a smooth exponential stellar profile. Therefore, Ref. [35] has redone the analysis of Ref. [34] with the profile described above. Also, Ref. [35] has scaled the radii of Ref. [42] to be consistent with the newer measurement of R_0 from Ref. [39]. Rescaling the total baryonic mass with our parameter f_b does not require redoing the analysis from Ref. [34], since the normalization cancels out, see e.g. their Eq. (3). Therefore, we can adjust the total baryonic mass while keeping the same rotation curve data.

4 Method and Data Analysis

Equations (1a) and (1b) describe only the core of the superfluid in the galactic center, not the non-superfluid phase at larger radii. However, our later estimate (see Section 5.3) shows that all data points fall well inside the superfluid core so that Eqs. (1a) and (1b) are sufficient to calculate the MW rotation curve in SFDM. As numerical values for the parameters in Eqs. (1a) and (1b) we use the fiducial values from Ref. [29]: $\beta = 2$, $\alpha = 5.7$, $m = 1$ eV, and $\Lambda = 0.05$ meV.

To integrate the equations, we assume axisymmetry and, as usual, parameterize it with cylindrical coordinates (R, z) . To numerically solve the equations summarized in Section 2, we run Mathematica 12's [43] PDESolve in the region $R^2 + z^2 < r_\infty^2$, $z > 0$ with $r_\infty = 115$ kpc. The value of r_∞ is chosen such that it is much larger than the size of the stellar and gas disks. It is possible to solve the equations only in the region $z > 0$ because in our approximation the Milky Way is symmetric under $z \rightarrow -z$. We calculate the rotation curve $v_c(R)$ as

$$v_c(R) = \sqrt{R \cdot |a_{\text{tot},R}(R, z=0)|}, \quad (8)$$

where $a_{\text{tot},R}$ is the R -component of the total acceleration \vec{a}_{tot} .

In the case of the full SFDM equations we use the boundary conditions

$$\partial_z \hat{\mu}|_{z=0} = 0, \quad (9a)$$

$$\partial_z \theta|_{z=0} = 0, \quad (9b)$$

$$\hat{\mu}|_{\sqrt{R^2+z^2}=r_\infty} = \mu_\infty, \quad (9c)$$

$$\theta|_{\sqrt{R^2+z^2}=r_\infty} = 0. \quad (9d)$$

The first two conditions encode the $z \rightarrow -z$ symmetry, the other two conditions impose spherical symmetry at r_∞ . This approximation of spherical symmetry is a good approximation in MOND and Newtonian gravity [44] which makes it reasonable that it is a good approximation here too.

For θ , the numerical value at r_∞ does not enter our equations so we just set it to zero. For $\hat{\mu}$, the numerical value at r_∞ determines the superfluid's density and therefore the superfluid's gravitational pull. This gravitational pull is typically subdominant in the

inner regions of a galaxy, but it is important at larger radii, e.g. to produce enough strong lensing [36]. Here, we choose the fixed value $\mu_\infty/m = 1.25 \cdot 10^{-7}$. As we will see below, this gives a subdominant but non-negligible contribution to the rotation curve at $R < 25$ kpc.

For the idealized MOND limit, we impose the boundary conditions

$$\partial_z \phi_N|_{z=0} = 0, \quad (10a)$$

$$\partial_z \bar{\theta}|_{z=0} = 0, \quad (10b)$$

$$\phi_N|_{\sqrt{R^2+z^2}=r_\infty} = 0, \quad (10c)$$

$$\bar{\theta}|_{\sqrt{R^2+z^2}=r_\infty} = 0. \quad (10d)$$

Since in this limit we neglect the superfluid's energy density ρ_{SF} , the numerical value of ϕ_N and $\bar{\theta}$ do not enter the equations and we can set both to zero.

The Mathematica function PDEsolve operates on a triangulation of the region described above. For this, we impose the following maximum areas of the triangular cells: For $R < 20$ kpc and $z < 0.5$ kpc, the maximum area is $(0.05 \text{ kpc})^2$. For $R < 40$ kpc and $z < 5$ kpc, it is $(0.2 \text{ kpc})^2$. For $R < 40$ kpc and $z < 10$ kpc, it is $(1 \text{ kpc})^2$. For $R < 40$ kpc and $z < 20$ kpc, it is $(2 \text{ kpc})^2$. Otherwise, the maximum area is $(10 \text{ kpc})^2$.

Eqs. (4b) and (1b) are of the form $\vec{\nabla}(g \vec{\nabla} \theta) = 4\pi G \rho_b$ with some function g . Therefore, they can be written as $\vec{\nabla}(g \vec{\nabla} \theta - \vec{\nabla} \phi_{N,b}) = 0$, where $\phi_{N,b}$ is the Newtonian gravitational potential produced by the baryons. This gives $g \vec{\nabla} \theta = \vec{\nabla} \phi_{N,b}$ up to a term that can be written as the curl of a vector field. Neglecting this term is often a reasonable approximation [45]. Below, we will refer to this approximation as the ‘no-curl-approximation’ and investigate how good an approximation to the full equations it is.

In the term of the form $\vec{\nabla}(g \vec{\nabla} \theta)$, g is not a smooth function for $\theta, \hat{\mu} \rightarrow 0$ due to the square roots in g . Unfortunately, this causes Mathematica's PDESolve to fail with the error “NDSolve::femdpop: The FEMStiffnessElements operator failed.” We work around this as follows. In the case of the full SFDM model, we rewrite the model, including the boundary conditions, in terms of $\hat{\mu}_{\text{temp}}(R, z) = \hat{\mu}(R, z) + \Delta \hat{\mu}$, where $\Delta \hat{\mu}$ is a constant. This suffices to make PDESolve solve the equations in terms of $\hat{\mu}_{\text{temp}}$. The solution for $\hat{\mu}_{\text{temp}}$ then gives a solution for $\hat{\mu}$ by subtracting $\Delta \hat{\mu}$. We verified that our results do not depend on the choice of $\Delta \hat{\mu}$. In the case of the idealized MOND limit, we simply shift $\sqrt{(\vec{\nabla} \bar{\theta})^2} \rightarrow \sqrt{C + (\vec{\nabla} \bar{\theta})^2}$ with a constant $C \ll (\vec{\nabla} \bar{\theta})^2$. We verified that $C \ll (\vec{\nabla} \bar{\theta})^2$ for the obtained solutions and that the choice of C does not affect our results.

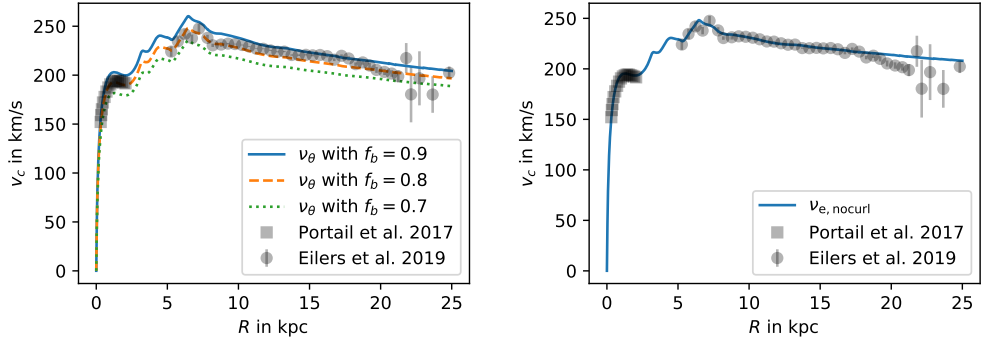


Figure 2: Left: Milky Way rotation curve in the idealized MOND-limit of SFDM for different values of f_b . Right: Milky Way rotation curve for MOND with the ν_e interpolation function in the no-curl-approximation (solid blue line). This reproduces Fig. 3 of Ref. [35] up to numerical differences and minor modifications described in Sec. 3. Also shown in both panels are the data from Ref. [34] (black dots) and Ref. [42] (black squares), both adjusted to match the assumptions of Ref. [35].

5 Results

5.1 Results for the idealized MOND regime

We begin with the results for the idealized MOND-limit of superfluid dark matter. The free parameter in this fit, f_b , is a factor for rescaling the total mass of baryons. In [46, 47] the stellar mass in the Milky Way was estimated with an observational uncertainty in the range of 10 – 20%. We therefore expect that the total mass of baryons has a similar observational uncertainty, which justifies allowing f_b to vary by this amount.

Fig. 2, left, shows the rotation curve of the Milky Way in terms of v_c from Eq. (8) in the MOND-limit in comparison with data for $f_b = 0.9, 0.8$, and 0.7 . The rotation curve data in this figure is that from Ref. [34] and Ref. [42] adjusted to match the assumptions of Ref. [35], as described in Sec. 3.

As one sees, to obtain a reasonable fit of the rotation curve data in the idealized MOND-limit of SFDM, we need 10 – 20 % less baryonic mass than the model of Ref. [35], i.e. $f_b \approx 0.8 – 0.9$. For $f_b = 0.8$, the total stellar mass in our model is $M_* = 4.98 \cdot 10^{10} M_\odot$. Ref. [46] estimates the MW's total stellar mass as $(5.43 \pm 0.57) \cdot 10^{10} M_\odot$ and Ref. [47] estimates $(6.08 \pm 1.14) \cdot 10^{10} M_\odot$. Thus, our value for M_* is relatively low, but still falls inside the error bars of Refs. [46, 47].

For reference, we further show in Fig. 2, right, the rotation curve obtained using the ν_e interpolation function and the no-curl-approximation for $f_b = 1$. This matches Fig. 3 of Ref. [35] up to numerical differences and the minor modifications described in Sec. 3. As discussed in Ref. [35], this model matches the data quite well.

There are three differences between SFDM's idealized MOND regime and the RAR as applied in Ref. [35]. First, the shapes of the interpolation functions ν_θ and ν_e differ. Second, the acceleration scales $a_{0,\theta}$ and $a_{0,e}$ differ. And third, Ref. [35] uses the no-curl-approximation while SFDM's idealized MOND-regime does not.

Using the no-curl-approximation induces a non-negligible error only at $R \lesssim 5$ kpc, as can be seen in Fig. 3, right. But even at $R \lesssim 5$ kpc, this error is only a few percent on v_c . Thus, the no-curl-approximation is not the main reason SFDM's idealized MOND regime requires significantly less baryonic mass than the ν_e -based model from Ref. [35].

The effect of the different acceleration scales $a_{0,\theta}$ and $a_{0,e}$ can be seen by using $a_{0,e}$ instead of $a_{0,\theta}$ in the equations of SFDM's idealized MOND regime. This is shown in Fig. 3, left. The effect of using $a_{0,e}$ instead of $a_{0,\theta}$ is larger at larger radii, where the additional MOND-like force begins to dominate. There, the larger acceleration scale increases v_c . Thus, the smaller acceleration scale $a_{0,\theta}$ helps SFDM's idealized MOND-limit to not require even less mass to fit the MW rotation curve.

This leaves the shape of ν_θ as the main reason that SFDM's idealized MOND regime requires less baryonic mass than the model from Ref. [35]. Concretely, ν_e approaches 1 at large baryonic accelerations much faster than ν_θ . Therefore, at large and intermediate accelerations, ν_θ produces a larger total acceleration than ν_e . As a result, less baryonic mass is needed to match the rotation curve data.

From Fig. 3, left, we can further see that SFDM's idealized MOND regime produces rotation curves not only with a different normalization compared to the model from Ref. [35], but also with a different shape. This is a consequence of both the different interpolation functions ν_e and ν_θ and the different acceleration scales $a_{0,\theta}$ and $a_{0,e}$. Below, we will see that the full SFDM equations can produce rotation curves that are closer to that of the ν_e -based model from Ref. [35].

The above results for SFDM's idealized MOND-limit may also apply to Covariant Emergent Gravity (CEG) [17] because CEG reduces to the same equations as SFDM's idealized MOND-limit, if we assume that only the 0-component of CEG's vector field u^μ is nonzero [36]. However, it is not clear whether or not this assumption holds for axisymmetric systems like the MW. Also, the numerical value of the acceleration scale may be different for CEG, see Ref. [36]. Thus, one should be careful when applying the above results to CEG.

5.2 Results for full SFDM

Fig. 4 compares the data of the Milky-Way rotation curve to the results from the full equations of superfluid dark matter. Again we have plotted the results for different values of the total mass of baryons, $f_b = 0.7, 0.8$, and 0.9 . As one sees, we get a good fit for f_b around 0.8, which is similar to our finding for the idealized MOND-limit discussed in the previous subsection.

In contrast to the idealized MOND-limit, however, for full superfluid dark matter the shape of the rotation curve is closer to the rotation curve obtained using the ν_e interpola-

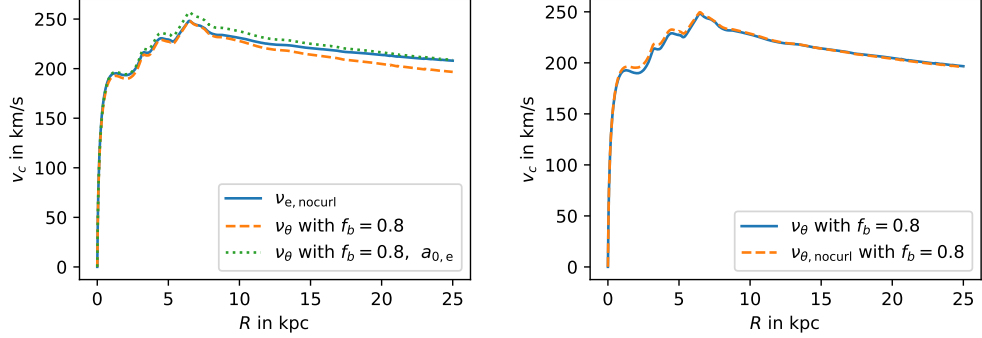


Figure 3: Left: Milky Way rotation curve in the idealized MOND regime of SFDM for $f_b = 0.8$ (dashed orange line), with $f_b = 0.8$ and $a_{0,e}$ instead of $a_{0,\theta}$ (dotted green line) compared with the ν_e rotation curve with $f_b = 1$ (solid blue line). Right: Milky Way rotation curve in the idealized MOND regime of SFDM for $f_b = 0.8$ (solid blue line) and for $f_b = 0.8$ in the no-curl-approximation (dashed orange line).

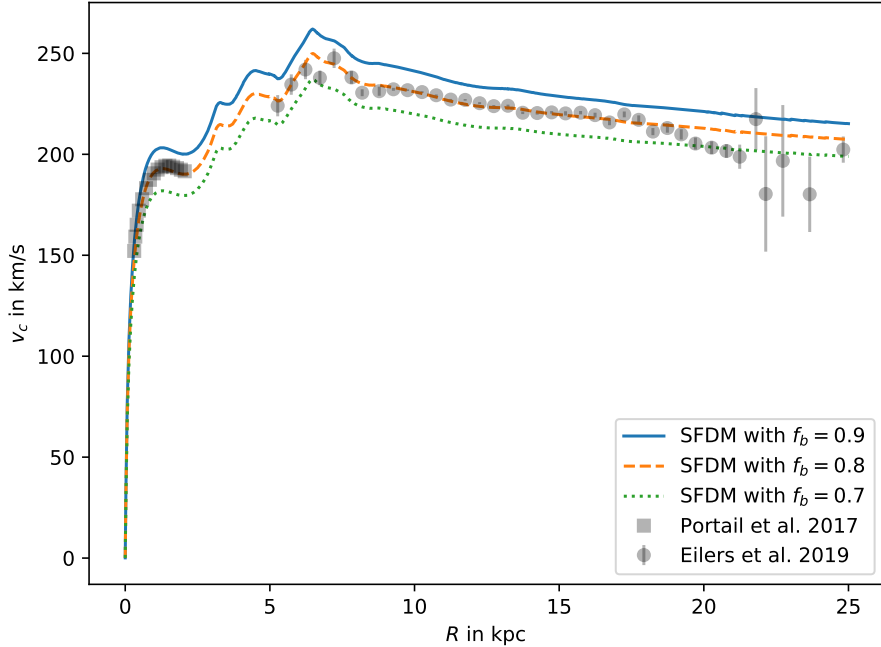


Figure 4: SFDM MW rotation curve for $f_b = 0.9$ (blue line), $f_b = 0.8$ (dashed orange line), and $f_b = 0.7$ (dotted green line). Also shown are the data from Ref. [34] (black dots) and Ref. [42] (black squares), both adjusted to match the assumptions of Ref. [35].

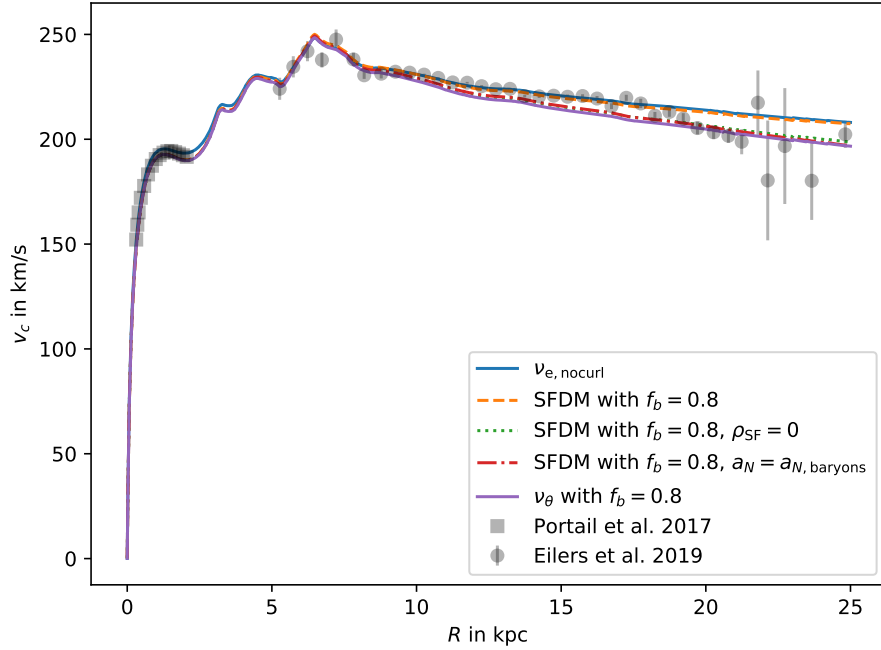


Figure 5: MW rotation curve from the ν_e -based model from Ref. [35] (solid blue line), from SFDM with $f_b = 0.8$ (dashed orange line), from SFDM's idealized MOND limit with $f_b = 0.8$ (solid purple line), and from SFDM with $f_b = 0.8$ with the superfluid's gravitational pull removed using two different methods. The first method is to set $\rho_{SF} = 0$ in SFDM's equations (dotted green line). The second method is to keep ρ_{SF} , but use only the baryonic Newtonian acceleration when calculating the rotation curve (dash-dotted red line). Also shown is the rotation curve data from Ref. [34, 42] in black, both adjusted to match the assumptions of Ref. [35].

tion function in Ref. [35]. This becomes clear from Fig. 5 which compares the rotation curve for SFDM with $f_b = 0.8$, the rotation curve obtained using the ν_e interpolation function with $f_b = 1$, and the rotation curve obtained in SFDM's idealized MOND-limit for $f_b = 0.8$.

This change of shape is due to the superfluid's gravitational pull as one can see by removing the superfluid's gravitational pull from the full SFDM model. The resulting rotation curves are very close to the rotation curve of SFDM's idealized MOND-limit, as shown in Fig. 5. For this, we have tried two different methods of removing the superfluid's gravitational pull from the full SFDM model, but both give similar results.

The first method is to simply set $\rho_{SF} = 0$. However, this does not just remove the superfluid's gravitational pull but also influences the θ equation of motion, i.e. the equation that determines the phonon force. This is because $\hat{\mu}$ enters the θ equation of

motion, but $\hat{\mu}$ is different with $\rho_{\text{SF}} = 0$ and $\rho_{\text{SF}} \neq 0$.

This motivates the second method of removing the superfluid's gravitational pull for which we solve the full SFDM-equations without removing ρ_{SF} , but when calculating the rotation curve we take $\vec{\nabla}\phi_{\text{N}}$ to be only the baryonic Newtonian gravitational pull, not the full Newtonian gravitational force including ρ_{SF} . This method is more ad-hoc, but has the advantage that the solution for θ is not affected.

However, as one sees in Fig. 5, the difference between both methods is small. Both methods give a rotation curve that is very close to that of the idealized MOND-limit. Therefore, we can unambiguously attribute the shape difference between the full model and the idealized MOND-limit to the superfluid's gravitational pull.

5.3 Estimates for the size of the superfluid core

In SFDM, galaxies contain a superfluid phase only at the centers of galaxies. In the outer parts of galaxies, the superfluid breaks down. The equations used above are valid only in the superfluid phase. Therefore, our results regarding the MW's rotation curve are valid only if the superfluid phase extends to $R > 25$ kpc. To check that it is consistent to use only the superfluid phase to fit the rotation curve data, we will now estimate the size of the MW's superfluid core.

Ref. [29] gives two different methods to estimate the size of the superfluid core for the case of spherical symmetry. The first method uses the so-called thermal radius R_{T} , the second method uses the so-called NFW radius R_{NFW} . Here, we will generalize both methods to axisymmetric situations. This will allow us to estimate the size of the superfluid's core in the R -direction ($R_{\text{T},R}$ and $R_{\text{NFW},R}$) and in the z -direction ($R_{\text{T},z}$ and $R_{\text{NFW},z}$).

We start with the thermal radius R_{T} . According to Sec. III of Ref. [29] this radius is determined by the relation

$$\Gamma = t_{\text{dyn}}^{-1}, \quad (11)$$

where Γ is the local self-interaction rate and t_{dyn} is the dynamical time. Here, $\Gamma = (\sigma/m)\mathcal{N}v\rho$, where σ is the self-interaction rate, $\mathcal{N} = (\rho/m)(2\pi/mv)^3$ is the Bose-degeneracy factor, and v is the average velocity of the particles. As in Ref. [29], we take $\sigma/m = 0.01 \text{ cm}^2/\text{g}$.

The assumption of spherical symmetry enters in the calculation of t_{dyn} and v . Specifically, Ref. [29] takes $t_{\text{dyn}} \approx r/v$ and $v^2 \approx r\partial_r\phi_{\text{N}}$ with the spherical radius r . For axisymmetric situations, we adjust this to be $t_{\text{dyn}} \approx R/v|_{z=0}$ and $v^2 \approx R\partial_R\phi_{\text{N}}|_{z=0}$ for the thermal radius $R_{\text{T},R}$ in R -direction and $t_{\text{dyn}} \approx z/v|_{R=0}$ and $v^2 \approx z\partial_z\phi_{\text{N}}|_{R=0}$ for the thermal radius $R_{\text{T},z}$ in z -direction.

For $f_b = 0.8$, we then get $R_{\text{T},R} = 112.10$ kpc and $R_{\text{T},z} = 112.12$ kpc. Thus, the superfluid's thermal radius is almost the same in R - and z -direction. This is not surprising since we assumed spherical symmetry at large radii. Also, $R_{\text{T},R}$ is much

larger than 25 kpc. This indicates that our above procedure for calculating the rotation curve is justified.

To estimate the NFW radius R_{NFW} , one assumes a superfluid in the centers of galaxies followed by an NFW profile at larger radii. The NFW radius R_{NFW} is then the radius at which the density and pressure of the superfluid core can be matched to the density and pressure of an NFW halo. Since the standard NFW profile is by definition spherically symmetric, the NFW radius is well-defined only when the superfluid core is spherically symmetric as well at the radius R_{NFW} . In our case, the superfluid will not be exactly spherically symmetric. However, the superfluid is approximately spherically symmetric at the NFW radius, if this radius is large enough. Thus, we define $R_{\text{NFW,R}}$ to be the value of R at $z = 0$, where the superfluid's density and pressure match those of the NFW halo, and $R_{\text{NFW,z}}$ to be the value of z at $R = 0$ where the pressure and density match. If the superfluid is approximately spherically symmetric at the NFW radii defined in this way, we will have $R_{\text{NFW,R}} \approx R_{\text{NFW,z}}$. The formulas for the pressure and density of the superfluid and the NFW halo can be taken directly from Ref. [29].

For $f_b = 0.8$, we find $R_{\text{NFW,R}} = 77.73$ kpc and $R_{\text{NFW,z}} = 77.72$ kpc. Thus, the superfluid seems to be sufficiently spherically symmetric at the NFW radius for our procedure to make sense. Just as the thermal radius $R_{\text{T,R}}$, the NFW radius $R_{\text{NFW,R}}$ is much larger than 25 kpc indicating that our above procedure for calculating the rotation curve is justified.

The difference between the NFW and the thermal radii is about 30 %. Therefore, we should take these radii as rough estimates rather than precise values. This is a limitation of our approach which assumes all of the dark matter particles to be in the condensed, superfluid phase. It may be possible to improve on this using a two-component approach where one component is in the superfluid phase and one component is in the normal, not-condensed phase [28, 29].

5.4 Estimate for the total dark matter mass

To estimate the total mass of dark matter in both the superfluid and normal phase, we use the density profile given by ρ_{SF} for $r < R_{\text{NFW,R}}$ and the NFW profile ρ_{NFW} matched at $r = R_{\text{NFW,R}}$ for $r > R_{\text{NFW,R}}$. With this, we can calculate the virial mass as

$$M_{200}^{\text{DM}} = 2\pi \iint_{R^2+z^2 < R_{\text{NFW,R}}^2} dR R dz \rho_{\text{SF}}(R, z) + 4\pi \int_{R_{\text{NFW,R}}}^{r_{200}} dr r^2 \rho_{\text{NFW}}(r). \quad (12)$$

Here, r_{200} is the spherical radius where the mean dark matter density drops below $200 \cdot 3H^2/(8\pi G)$, where H is the Hubble constant. For $H = 67.3 \text{ km}/(\text{s} \cdot \text{Mpc})$, we then find $M_{200}^{\text{DM}} = 4.2 \cdot 10^{12} M_{\odot}$. For comparison, the NFW fit from Ref. [34] gives $M_{200}^{\text{DM}} = (7.25 \pm 0.26) \cdot 10^{11} M_{\odot}$ which is significantly lower. However, our value for M_{200}^{DM} depends heavily on the choice of μ_{∞} , as will be discussed in the next section.

6 Discussion

The results for superfluid dark matter that we presented above depend on a free constant, the initial value of the chemical potential μ_∞ . In SFDM, the thermal and NFW radii depend on the choice of μ_∞ , since μ_∞ determines the superfluid's density and pressure profiles. The rotation curve in the range $R < 25$ kpc is not very sensitive to μ_∞ but, as we noted in Section 5.4, the dark matter halo at larger radii depends heavily on μ_∞ . A similar observation was previously discussed in Secs. 6.2 and 6.3 of Ref. [36].

To investigate this dependence on μ_∞ , we also solved the SFDM-equations with μ_∞ smaller by a factor of 30. We found that this changes the rotation curve for $R < 25$ kpc by less than 1%. However, it lowers the thermal and the NFW radii by roughly 10%. With the smaller value of μ_∞ we have $R_T \approx 97$ kpc and $R_{\text{NFW}} \approx 70$ kpc. The effect on the virial dark matter mass M_{200}^{DM} is even bigger. We find $M_{200}^{\text{DM}} = 1.8 \cdot 10^{12} M_\odot$ which is less than half of the virial mass obtained with the original μ_∞ .

In this present work, we are concerned with the rotation curve at $R < 25$ kpc. In this range, the rotation curve depends only weakly on μ_∞ . It then suffices to confirm that our choice of μ_∞ gives a superfluid core extending to $R > 25$ kpc as well as a reasonable rotation curve. As discussed in the previous section, this is indeed the case. The precise choice of μ_∞ would, however, become important for comparison to data at larger radii.

It must further be mentioned that we here compared the model of SFDM to rotation curve data, but even in the Milky-Way this is not the only available data. There may be additional constraints from vertical acceleration measurements as discussed in [48, 49]. These constraints are a serious problem for MOND. However, for SFDM they are not necessarily problematic. Because the superfluid interacts with the baryons, it should strictly speaking also rotate, which quite plausibly affects the vertical gradient of the phonon-force. However, we do not have a theoretical framework to handle a rotating two-component fluid in a gravitational potential, so, unfortunately, we cannot address this interesting constraint here.

It also should be noted that while we fitted f_b , it might make more physical sense to instead fit the parameters of the SFDM-model. There is little reason to doubt this is possible because the model has four free parameters, whereas we were able to fit the data with only one free parameter. However, attempting to fit the SFDM parameters to the MW data makes no sense in isolation because changing the parameters will affect the goodness-of-fit to other astrophysical data. To address this point, one would need to do a global fit to all available data to identify the best-fit parameters, but this is beyond the scope of this present work.

7 Conclusion

We have shown here that superfluid dark matter which mimics MOND with a phonon-force has no trouble explaining the newest data for the Milky-Way rotation curve. Su-

perfluid dark matter provides a fit of the rotation curve that is similarly good as MOND, provided that the total baryonic mass is 10 – 20% less than the current estimates of the stellar mass. This amount of baryonic mass in the Milky Way is currently well within measurement uncertainty. However, in the future, with better measurements of the Milky-Way’s baryonic mass, the here presented result may enable us to tell apart superfluid dark matter from MOND.

Acknowledgements

We thank Stacy McGaugh for helpful discussion and for kindly providing the data used in our analysis. SH gratefully acknowledges support from the German Research Foundation (DFG).

References

- [1] W. J. G. de Blok, “The Core-Cusp Problem”, *Advances in Astronomy* **2010**, 789293, 789293 (2010), arXiv:0910.3538.
- [2] M. Mateo, “Dwarf galaxies of the Local Group”, *Ann. Rev. Astron. Astrophys.* **36**, 435 (1998), arXiv:astro-ph/9810070.
- [3] B. Moore, S. Ghigna, F. Governato, G. Lake, T. R. Quinn, J. Stadel, and P. Tozzi, “Dark matter substructure within galactic halos”, *Astrophys. J.* **524**, L19 (1999), arXiv:astro-ph/9907411.
- [4] A. Del Popolo and M. Le Delliou, “Small scale problems of the Λ CDM model: a short review”, *Galaxies* **5**, 17 (2017), arXiv:1606.07790.
- [5] R. B. Tully and J. R. Fisher, “A New method of determining distances to galaxies”, *Astron. Astrophys.* **54**, 661 (1977).
- [6] F. Lelli, S. S. McGaugh, J. M. Schombert, and M. S. Pawlowski, “One Law to Rule Them All: The Radial Acceleration Relation of Galaxies”, *Astrophys. J.* **836**, 152, 152 (2017), arXiv:1610.08981.
- [7] M. Tanabashi et al. (Particle Data Group Collaboration), “Review of Particle Physics”, *Phys. Rev.* **D98**, 030001 (2018).
- [8] M. Milgrom, “A Modification of the Newtonian dynamics as a possible alternative to the hidden mass hypothesis”, *Astrophys. J.* **270**, 365 (1983).
- [9] M. Milgrom, “A modification of the Newtonian dynamics: implications for galaxy systems”, *Astrophys. J.* **270**, 384 (1983).
- [10] J. Bekenstein and M. Milgrom, “Does the missing mass problem signal the breakdown of Newtonian gravity?”, *Astrophys. J.* **286**, 7 (1984).

- [11] J. D. Bekenstein, “Relativistic gravitation theory for the MOND paradigm”, *Phys. Rev.* **D70**, [Erratum: *Phys. Rev.* D71, 069901 (2005)], 083509 (2004), arXiv:astro-ph/0403694.
- [12] M. Milgrom, “Quasi-linear formulation of MOND”, *Mon. Not. Roy. Astron. Soc.* **403**, 886 (2010), arXiv:0911.5464.
- [13] T. G. Zlosnik, P. G. Ferreira, and G. D. Starkman, “Modifying gravity with the Aether: An alternative to Dark Matter”, *Phys. Rev.* **D75**, 044017 (2007), arXiv:astro-ph/0607411.
- [14] M. Milgrom, “Bimetric MOND gravity”, *Phys. Rev.* **D80**, 123536 (2009), arXiv:0912.0790.
- [15] C. Deffayet, G. Esposito-Farese, and R. P. Woodard, “Nonlocal metric formulations of MOND with sufficient lensing”, *Phys. Rev.* **D84**, 124054 (2011), arXiv:1106.4984.
- [16] L. Blanchet and L. Heisenberg, “Dipolar Dark Matter with Massive Bigravity”, *JCAP* **1512**, 026 (2015), arXiv:1505.05146.
- [17] S. Hossenfelder, “Covariant version of Verlinde’s emergent gravity”, *Phys. Rev.* **D95**, 124018 (2017), arXiv:1703.01415.
- [18] P. Sikivie and Q. Yang, “Bose-Einstein Condensation of Dark Matter Axions”, *Phys. Rev. Lett.* **103**, 111301 (2009), arXiv:0901.1106.
- [19] T. Noumi, K. Saikawa, R. Sato, and M. Yamaguchi, “Effective gravitational interactions of dark matter axions”, *Phys. Rev.* **D89**, 065012 (2014), arXiv:1310.0167.
- [20] S. Davidson and M. Elmer, “Bose Einstein condensation of the classical axion field in cosmology?”, *JCAP* **1312**, 034 (2013), arXiv:1307.8024.
- [21] H. J. de Vega and N. G. Sanchez, “Galaxy phase-space density data exclude Bose-Einstein condensate Axion Dark Matter”, (2014), arXiv:1401.1214.
- [22] S. Davidson, “Axions: Bose Einstein Condensate or Classical Field?”, *Astropart. Phys.* **65**, 101 (2015), arXiv:1405.1139.
- [23] A. H. Guth, M. P. Hertzberg, and C. Prescod-Weinstein, “Do Dark Matter Axions Form a Condensate with Long-Range Correlation?”, *Phys. Rev.* **D92**, 103513 (2015), arXiv:1412.5930.
- [24] A. Aguirre and A. Diez-Tejedor, “Asymmetric condensed dark matter”, *JCAP* **1604**, 019 (2016), arXiv:1502.07354.
- [25] P. S. B. Dev, M. Lindner, and S. Ohmer, “Gravitational waves as a new probe of Bose-Einstein condensate Dark Matter”, *Phys. Lett.* **B773**, 219 (2017), arXiv:1609.03939.
- [26] J. Eby, M. Ma, P. Suranyi, and L. C. R. Wijewardhana, “Decay of Ultralight Axion Condensates”, *JHEP* **01**, 066 (2018), arXiv:1705.05385.
- [27] S. Sarkar, C. Vaz, and L. C. R. Wijewardhana, “Gravitationally Bound Bose Condensates with Rotation”, *Phys. Rev.* **D97**, 103022 (2018), arXiv:1711.01219.

- [28] L. Berezhiani and J. Khoury, “Theory of dark matter superfluidity”, *Phys. Rev. D* **92**, 103510, 103510 (2015), arXiv:1507.01019.
- [29] L. Berezhiani, B. Famaey, and J. Khoury, “Phenomenological consequences of superfluid dark matter with baryon-phonon coupling”, *JCAP* **1809**, 021 (2018), arXiv:1711.05748.
- [30] B. P. Abbott et al., “Multi-messenger Observations of a Binary Neutron Star Merger”, *Astrophys. J.* **848**, L12 (2017), arXiv:1710.05833.
- [31] S. Hossenfelder and T. Miste, “Strong lensing with superfluid dark matter”, *JCAP* **1902**, 001 (2019), arXiv:1809.00840.
- [32] E. P. Verlinde, “Emergent Gravity and the Dark Universe”, *SciPost Phys.* **2**, 016 (2017), arXiv:1611.02269.
- [33] J. Bland-Hawthorn and O. Gerhard, “The galaxy in context: structural, kinematic, and integrated properties”, *Annual Review of Astronomy and Astrophysics* **54**, 529 (2016), eprint: <https://doi.org/10.1146/annurev-astro-081915-023441>.
- [34] A.-C. Eilers, D. W. Hogg, H.-W. Rix, and M. K. Ness, “The Circular Velocity Curve of the Milky Way from 5 to 25 kpc”, *Astrophys. J.* **871**, 120, 120 (2019), arXiv:1810.09466.
- [35] S. McGaugh, “The Imprint of Spiral Arms on the Galactic Rotation Curve”, *Astrophys. J.* **885**, 87 (2019), arXiv:1909.11158.
- [36] S. Hossenfelder and T. Miste, “The redshift-dependence of radial acceleration: Modified gravity versus particle dark matter”, *International Journal of Modern Physics D* **27**, 1847010, 1847010 (2018), arXiv:1803.08683.
- [37] J. Bovy and H.-W. Rix, “A Direct Dynamical Measurement of the Milky Way’s Disk Surface Density Profile, Disk Scale Length, and Dark Matter Profile at 4 kpc $\lesssim R \lesssim$ 9 kpc”, *Astrophys. J.* **779**, 115, 115 (2013), arXiv:1309.0809.
- [38] R. P. Olling and M. R. Merrifield, “Luminous and dark matter in the Milky Way”, *Monthly Notices of the Royal Astronomical Society* **326**, 164 (2001), arXiv:astro-ph/0104465.
- [39] Gravity Collaboration, “Detection of the gravitational redshift in the orbit of the star S2 near the Galactic centre massive black hole”, *A & A* **615**, L15, L15 (2018), arXiv:1807.09409.
- [40] S. S. McGaugh, “Milky Way Mass Models and MOND”, *Astrophys. J.* **683**, 137 (2008), arXiv:0804.1314.
- [41] K. C. Freeman, “On the Disks of Spiral and S0 Galaxies”, *Astrophys. J.* **160**, 811 (1970).

- [42] M. Portail, O. Gerhard, C. Wegg, and M. Ness, “Dynamical modelling of the galactic bulge and bar: the Milky Way's pattern speed, stellar and dark matter mass distribution”, *Monthly Notices of the Royal Astronomical Society* **465**, 1621 (2017), arXiv:1608.07954.
- [43] Wolfram Research, Inc., *Mathematica, Version 12*.
- [44] M. Milgrom, “Solutions for the Modified Newtonian Dynamics Field Equation”, *Astrophys. J.* **302**, 617 (1986).
- [45] R. Brada and M. Milgrom, “Exact solutions and approximations of MOND fields of disc galaxies”, *Monthly Notices of the Royal Astronomical Society* **276**, 453 (1995).
- [46] P. J. McMillan, “The mass distribution and gravitational potential of the Milky Way”, *Monthly Notices of the Royal Astronomical Society* **465**, 76 (2017), arXiv:1608.00971.
- [47] T. C. Licquia and J. A. Newman, “Improved Estimates of the Milky Way's Stellar Mass and Star Formation Rate from Hierarchical Bayesian Meta-Analysis”, *Astrophys. J.* **806**, 96, 96 (2015), arXiv:1407.1078.
- [48] M. Lisanti, M. Moschella, N. J. Outmezguine, and O. Slone, “Testing dark matter and modifications to gravity using local Milky Way observables”, *Phys. Rev. D* **100**, 083009, 083009 (2019), arXiv:1812.08169.
- [49] M. Lisanti, M. Moschella, N. J. Outmezguine, and O. Slone, “The Inconsistency of Superfluid Dark Matter with Milky Way Dynamics”, *arXiv e-prints*, arXiv:1911.12365 (2019), arXiv:1911.12365.